IET Nanobiotechnology

Research Article

IET Journals
The Institution of Engineering and Technology

In situ synthesised TiO_2-chitosan-chondroitin 4–sulphate nanocomposites for bone implant applications

ISSN 1751-8741
Received on 23rd March 2015
Accepted on 26th June 2015
doi: 10.1049/iet-nbt.2015.0023
www.ietdl.org

Martina Jenitha Alex, Prabu Periasamy ✉, Kalirajan Mohan, Sankar Sekar, Kavitha Kandiah Suriya Prabha, Rajendran Venkatachalam

Centre for Nano Science and Technology, K S Rangasamy College of Technology, Tiruchengode-637 215, Tamil Nadu, India
✉ *E-mail: prabukrp@gmail.com*

Abstract: The artificial materials for bone implant applications are gaining more importance in the recent years. The series titania-chitosan-chondroitin 4–sulphate nanocomposites of three different concentrations (2:1:*x*, where *x*- 0.125, 0.25, 0.5) have been synthesised by *in situ* sol–gel method and characterised by various techniques. The particle size of the nanocomposites ranges from 30–50 nm. The bioactivity, swelling nature, and the antimicrobial nature of the nanocomposites were investigated. The swelling ability and bioactivity of the composites is significantly greater and they possess high zone of inhibition against the microorganisms such as *Staphylococcus aureus* and *Escherichia coli*. The cell viability of the nanocomposites were evaluated by using MG-63 and observed the composites possess high cell viability at low concentration. The excellent bioactivity and biocompatibility makes these nanocomposites a promising biomaterial for bone implant applications.

1 Introduction

Bone tissue engineering has evolved the means to develop the bone grafts to repair the damaged tissue and maintain the function of the natural bone using effective biomaterials [1, 2]. Biomaterials used in bone tissue engineering should possess excellent bioactivity, biocompatibility and mechanical properties [3]. Among many tissues in the body, bone has the highest potential for regeneration and hence, the accumulating knowledge in bone tissue engineering will lead to the design of bone such as material with predetermined properties [4]. Nanocomposites of different materials show unique with synergistic properties and acts as an effective biomaterial in different medical applications such as bone tissue engineering, dental implants [5–7], drug delivery [8, 9], gene therapy [10] and cartilage tissue engineering [11] etc., which promotes the cell growth and degrade after the certain period of implantation. Nano titania has received considerable attention as a biomaterial due to its excellent biocompatibility and unique physic-chemical properties [12, 13]. TiO_2 forms bone such as apatite and also reduces the corrosion in implants through the formation of oxide layer in their surroundings [14]. The toxicological aspects of TiO_2 limit its use in biomedical applications which can be overcome by preparing the nanocomposites with the biodegradable and biocompatible natural polymers such as chitosan (Ch), collagen, cellulose, and extra cellular matrix (ECM) proteins [15].

Chitosan is the second abundant biopolymer in nature after cellulose has been extensively used in medical applications because of its favourable biological properties such as biodegradability, superior biocompatibility, non-toxicity [16, 17] and antimicrobial properties [18]. Ch the derivative of deacetyled chitin, consists of copolymers of glucosamine and *N* acetyl glucosamine which are similar to glycosaminoglycans the components of extracellular matrix [19, 20]. Ch can be moulded in various shapes and interact with living cells through react amine and hydroxyl groups which is used to modulate integration in host tissue [21–23]. This property makes chitosan an extremely important biomaterial for bone tissue engineering applications. Rapid degradability and hydrophobic property of chitosan often leads to the problem such as poor cell attachment [24, 25]. To overcome this problem, hydrophilic polymer such as chondroitin 4–sulphate (Cs) is added along with chitosan, which enhances the performance of chitosan which in turn increases the hydrophilicity and biocompatibility [26].

Chondroitin 4–sulphate is also naturally occurring glycosaminoglycans present in ECM of cartilage and which confers cartilage desired mechanical properties. Cs is an anionic polyelectrolyte consisting of repeating disaccharide units of β −1, 4 linked D-gluconicacid and β–1, 3 *N* acetyl galactosamine [27]. Ch and Cs contain hydrophilic polymer network that can absorb much more water than their own weight and enhances the growth factors [28, 29]. Further, the formation of highly cross linked network structure increases the mechanical strength and stability of the Cs [30]. Ch and Cs complex bound with TiO_2 improves the biological acceptance of Ti based implants. Inflammatory reactions at injury sites are reduced by Cs due to the accelerated metabolism of cells and the ability to sustain a normal microenvironment for cell growth [31]. Compared with the conventional synthesis method, TiO_2-Ch-Cs nanocomposites with homogeneous dispersion of particle are obtained by *in situ* sol–gel mediated synthesis [32] may help to enhance the biological, mechanical properties and avoids toxicity promotes cell growth factors of bone [33].

The objective of this present work is to synthesis TiO_2-Ch-Cs nanocomposites by *in situ* method with different compositions of chondroitin sulphate. The nanocomposites powders are analysed through various characterisation techniques and *in vitro* studies to explore the swelling behaviour, bioactivity, antibacterial activity and biocompatability.

2 Materials and methods

2.1 Materials

The raw materials such as, Chitosan from crab shells (Catalog No.: 41, 796–3), chondroitin 4–sulphate a sodium salt from bovine trachea (Catalog No.: C 9819), were purchased from Sigma-Aldrich (Germany). Eagle's Minimum Essential Medium (EMEM, Catalog No.: 30–2003) containing 10% foetal bovine serum (FBS) and MTT assay (3-(4, 5-dimethylthiazole-2-yl)-2–

5-diphenyl tetrazolium bromide) kit for cell proliferation analysis (catalog No.: 070M61471) were obtained from Sigma-Aldrich (USA). MG-63 cell line (ATCC CRL-1427) was supplied by National center for cell science, Pune, India. The other chemicals Titanium isopropoxide $Ti(OC_3H_7)_4$ (Catalog No.: 205273) Isopropyl alcohol ($CH_3CHOHCH_3$), acetyl acetone ($C_5H_8O_2$) etc., were purchased from Sigma-Aldrich and Merk, Mumbai were of analytical grade and used as received.

2.2 Preparation of nanocomposites

Pure TiO_2 was synthesised from using precipitation method [34] and the TiO_2-Ch-Cs nanocomposites were synthesised by *in situ* sol–gel method [35]. TiO_2-Ch-Cs nanocomposites with three different chondroitin 4–sulphate is prepared in the following ratio (2/1/0.125, 2/1/0.25, 2/1/0.5 hereafter termed as CTC 1, CTC 2, CTC 3 respectively). Titanium isopropoxide diluted with isopropyl alcohol followed by addition of acetyl acetone (to control hydrolysis) in the molar ratio 1:4:0.7. After 1 h, chitosan (1 g L^{-1}) was dissolved in 2% acetic acid, and chondroitin 4–sulphate was dissolved in deionised water at different concentrations (0.125, 0.25, 0.5 g L^{-1}) separately. The prepared solutions of chitosan and chondroitin4–sulphate were added drop by drop simultaneously to the diluted titanium isopropoxide under vigorous stirring. At certain point, the solutions reach the semi-solid state which was then dried at 50°C for 12–24 h to evaporate the solvent. The dried samples were grinded into powders and then stored in desiccators to avoid agglomeration.

2.3 Characterisation

The crystalline nature and phase identification were carried out with an X-ray diffractometer (XRD) (X'Pert pro; PANalytical, Netherland) using CuKα as radiation source (wavelength $\lambda =$ 0.15406). Fourier transform infrared (FTIR) spectra of each sample were analysed using spectrometer (spectrum 100; PerkinElmer, USA) by passing infrared radiation through the sample. The surface morphology and elemental composition of prepared nanocomposites were examined using scanning electron microscope combined with energy dispersive X-ray spectroscopy (SEM-EDX) (JSM-6390LV, Japan) and X-ray fluorescence spectroscopy (XRF) (EDX-720; Shimadzu, Japan). Each sample was mounted and sputter coated with gold palladium prior to examination by SEM. The particle size of the sample was examined using TEM (CM 200; Philips, USA). The sample was prepared by dropping TiO_2-Ch-Cs aqueous suspension onto a copper grid covered with a thin carbon layer for analysis of particle size.

2.3.1 Mechanical characterisation: The mechanical properties of all the samples were examined using nanoindentation Triboindenter (Quasi-static nanoindentation, TI 700 ubi; Hysitron Inc, USA). The nanohardness and the young's modulus of the nanocomposites were measured under the room temperature. The samples were pressed in pellets and mounted on Triboindenter for the mechanical analysis.

2.4 Antimicrobial activity

The antibacterial activity of CTC nanocomposites was obtained against the clinical isolates of bone infecting organisms such as *Staphylococcus aureus* (ATCC 25923) and *Escherichia coli* (ATCC 25922) which were purchased from Microbial type culture collection and gene bank Chandigarh, India. The bacteria obtained were cultured in 2 ml nutrient broth overnight and then transferred to 100 ml nutrient broth and incubated at 37°C for 3–4 h. The newly grown cell suspension (0.1 ml) was spread in a Muller–Hinton agar plate. The disc diffusion method was used to analyse the antibacterial activity of the prepared nanocomposites [36].

2.5 In vitro *bioactivity*

The *in vitro* bioactivity and an apatite forming ability of the prepared samples were explored by soaking them into a 1.5 simulated body fluid (1.5 SBF). The 1.5 SBF solution was prepared by dissolving analytical grade chemicals (NaCl, $NaHCO_3$, KCl, K_2PO_4.3H2O, $MgCl_2.6H_2O$, 1.0M HCl, $CaCl_2$, Na_2SO_4 and $(HOCH_2)3CNH2$) in deionised water [37]. The ionic concentration of the SBF had a similar composition to the human blood plasma and the solution was buffered at pH 7.4 using Tris and HCl. The prepared samples were immersed in 1.5 SBF solutions of 1.5 gL^{-1} and incubated for 21 days at 37°C. After incubation the samples were removed from the fluid dried and weighted. The dry weight of the pellets were measured and then compared with the initial weight. The ionic concentration Ca and P were determined by XRF.

2.6 In vitro *swelling study*

The initial weight of the sample was measured before the samples were immersed in phosphate buffer solution (PBS) solution. The samples were soaked in (PBS) at pH 7.4 and incubated at 37°C for 7 days to explore the swelling behaviour of them [38]. At defined days say 1, 4 and 7 the buffer was carefully removed using filter paper and the wet weight of the sample was measured. The swelling ratio was calculated by using the following equation

$$w(\%) = \frac{W_i - W_o}{W_o} \times 100 \quad (1)$$

where W is the swelling ratio of the sample, W_i the initial weight of the sample and W_o the wet weight of the PBS immersed sample.

2.7 Cytotoxicity

The effects of CTC nanocomposites on cytotoxicity were determined using colorimetric MTT assay [39]. The MTT assay is the non-radioactive assay for measuring cell cytotoxicity or viability. MG 63 cells were grown in EMEM medium containing 5% FBS, sodium pyruvate, 0.15% sodium bicarbonate, non-essential amino acids, 2 mM glutamine, penicillin (100 µg ml^{-1}) and streptomycin (100 µg ml^{-1}). The cell suspension were seeded into 96 well micro titrate plate at a density of 1×10^3 cells per well and allowed to adhere for 24 h. The nanocomposites of three different concentrations 31.25, 65.5, 125, 250 µg ml^{-1} were added to each well and incubated at 37°C for 48 h. The morphological changes of MG-63 cell lines for every 12 h was observed using inverted tissue culture binocular microscope. MTT solution (80 µg ml^{-1}) was added to the sample to explore the mitochondrial damage of the cells depending upon the colour formation and optical density (OD) at 570 nm. OD was measured at 570 nm. The percentage of cell viability was calculated using the following formula.

$$\frac{\text{OD of nanoparticles treated cell}}{\text{OD of the control cells}} \times 100 \quad (2)$$

The cell viability experiments were performed in triplicate ($n = 3$) and repeated three times. Statistical difference between the means in the measured data was determined by Tukey's least significant difference and Duncan's post hoc tests. Statistical analysis was carried out one way analysis of variance using SPSS software. A value of $p < 0.05$ was considered statistically significant.

3 Results and discussion

3.1 X-Ray diffraction

The internal structure such as the crystalline phase and crystallite size of nanocomposites were obtained by the X-ray diffraction analysis. The diffraction peaks of the nanocomposites is shown in Fig. 1*a* The XRD results of the nanocomposite shows the presence of

IET Nanobiotechnol., 2016, Vol. 10, Iss. 3, pp. 107–113

tetragonal anatase phase of TiO_2 with highest peak at 27.4° (JCPDS 21–1276). The inclusion of Ch and Cs does not induce any other peaks but as the concentration Cs increases the intensity of the peaks decreases gradually. The average crystallite size of the CTC 1, CTC 2, and CTC 3 are 4.81 nm, 4.08 nm, 8.05 nm respectively. As the concentration of the chondroitin sulphate increases the crystallite size and amorphous nature of the material also increases.

3.2 Fourier transform infrared spectroscopy (FT-IR)

FT-IR spectra of the nanocomposites are shown in the Fig. 2*a*. The Ti-O-Ti stretching is obtained at 900–400 cm^{-1}. The peaks observed at 1029, 1154 cm^{-1} indicate the bending modes of Ti-O-C and the stretching bands of C-O-C respectively. Bending vibrations of N-H is confirmed by the corresponding peak at 1618 cm^{-1}. The characteristic peaks observed at 1200–800, 3400 cm^{-1} reveals the presence of polysaccharides and the presence of sulphate groups [40] which confirms the presence of TiO_2-Chitosan-Chondroitin sulphate nanocomposites. Ti-OH stretching at 1287 is the constructive site for the accumulation of ions and the formation of HAp layer. The peak at 1655 attributes to the stretching vibrations of amide (I) band. The sharp peaks at 1409 cm^{-1} are assigned to the CH_3 symmetrical deformation mode and 1074 cm^{-1} indicates the C-O stretching vibrations [41].

3.3 Scanning electron microscopy

The SEM images of the prepared nanocomposites confirm the irregular surface morphology of CTC nanocomposites. From our previous studies, the pure TiO_2 shows the spherical morphology [34]. In contrast, the inclusion of chitosan and chondroitin 4–sulphate shows the irregular morphology. As the concentration of the chondroitin 4–sulphate increases in nanocomposites the agglomerated irregular morphology also increases due to the strong interaction between two oppositely charged polysaccharides [9]. The chemical composition of the samples were obtained by EDX in Fig. 3 confirms the purity of the nanocomposites.

3.4 Transmission electron microscopy

The TEM images of the prepared TiO_2-CH-CS nanocomposites were shown in Fig. 4 The morphology of the CTC nanocomposites shows agglomerated irregular shape as observed in SEM results. The particle size of CTC 1, CTC 2, CTC 3 is 38.72, 32.44, 25.32 nm respectively. As the concentration of chondroitin 4–sulphate increases the particle size decreases (Table 1).

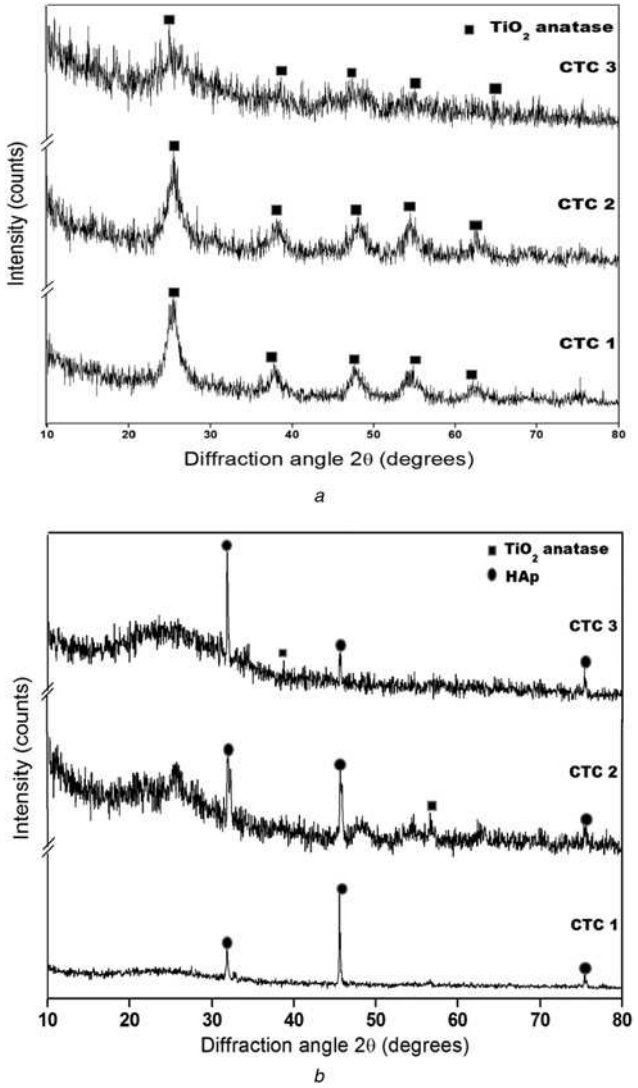

Fig. 1 *X-ray diffraction pattern of a series of TiO_2-chitosan-chondroitin 4–sulphate nanocomposite for bioactivity*

a before *in vitro* study
b after *in vitro* study

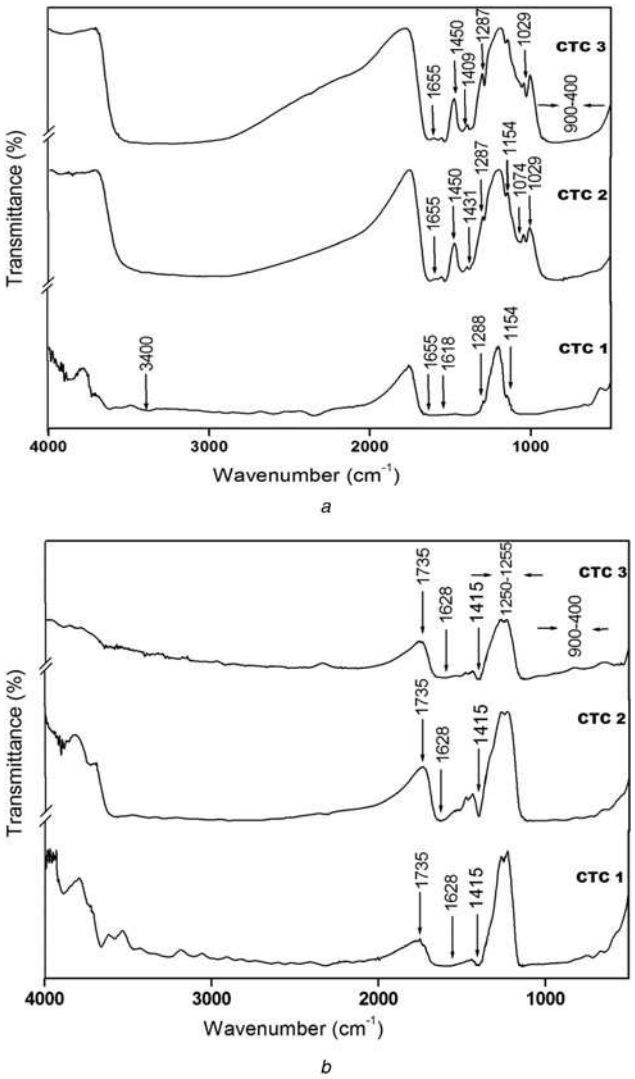

Fig. 2 *FTIR spectra of TiO_2-chitosan-chondroitin 4–sulphate nanocomposites for bioactivity*

a before *in vitro* study
b after *in vitro* study

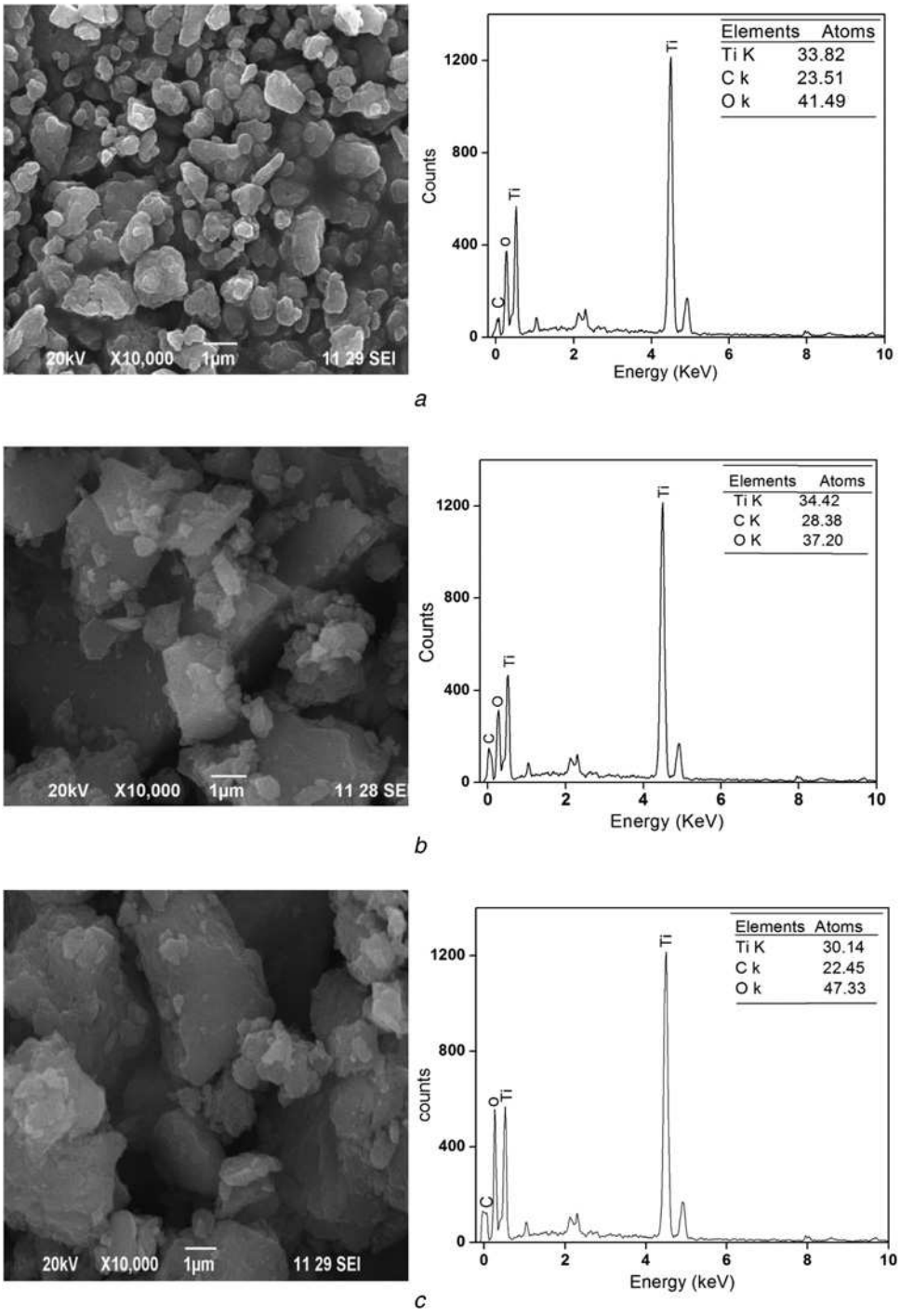

Fig. 3 *SEM-EDX images of TiO_2- chitosan- chondroitin 4–sulphate nanocomposite*

a CTC 1
b CTC 2
c CTC 3

3.5 Nanoindentation

Mechanical strength of the nanocomposite is evaluated by nanoindentation system and as given in Fig. 5. The measured nanohardness of nanocomposites are 1.22, 1.13 and 08.61 GPa respectively and Young's moduli are 19.07, 13.68 and 12.78 respectivlely for the CTC 1, CTC 2 and CTC 3 nanosamples. It shows that decrease in hardness and Young's moduli are observed while increasing the concentration of the chondroitin 4–sulphate. The desirable mechanical strength is essential to support the osteoconduction and cell growth, which is further enhanced by attachment and load bearing behaviour [42]. The prepared composite CTC 1 is considered as a good strength biomaterial for bone regeneration application than the CTC 2 and CTC 3.

3.6 In vitro *bioactivity*

The CTC nanocomposites shows increased bioactivity compared with the control. The characterisation results such as XRD and FT-IR shows the increased hydroxyapatite layer formation in the nanocomposites. The XRD results of the nanocomposites after immersion in 1.5 SBF is shown in Fig. 1*b* confirms the deposited calcium and phosphate to be hydroxyapatite with the diffraction

IET Nanobiotechnol., 2016, Vol. 10, Iss. 3, pp. 107–113

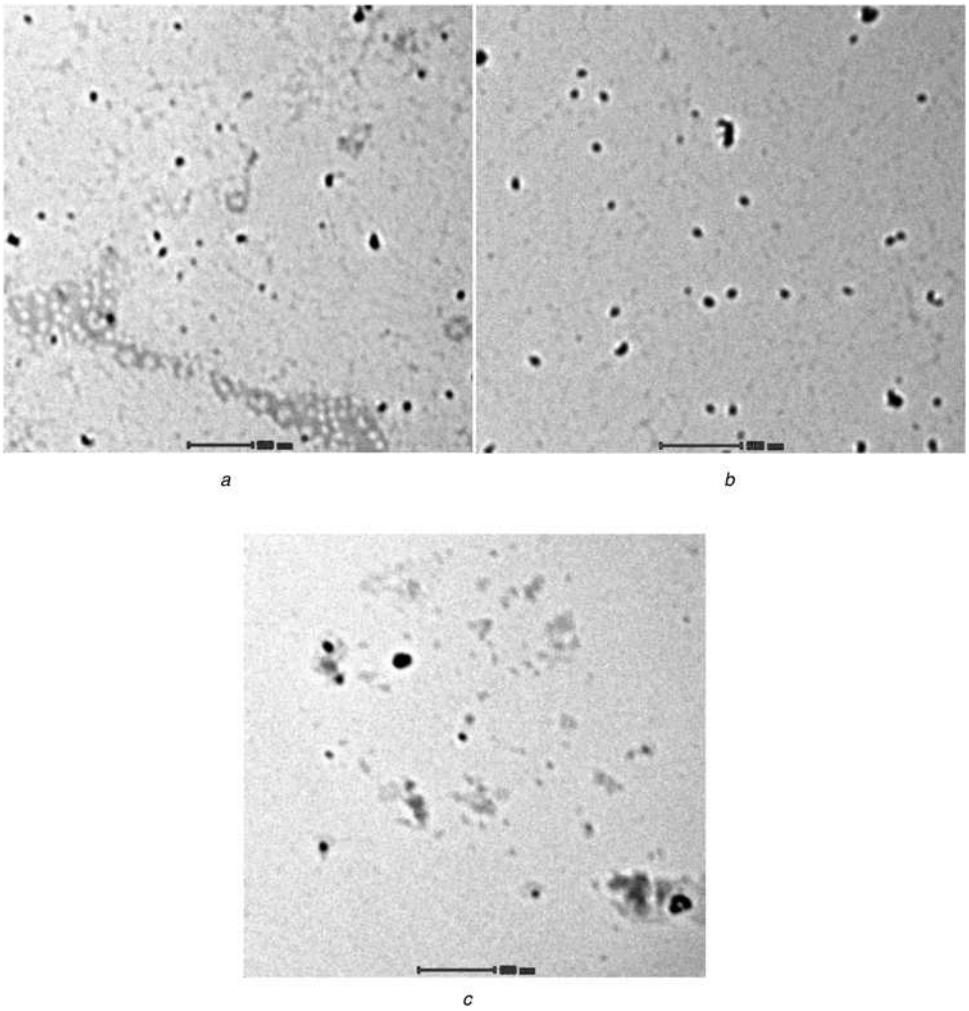

Fig. 4 *TEM images of TiO_2-chitosan- chondroitin 4–sulphate nanocomposite*

a CTC 1
b CTC 2
c CTC 3

peaks and their corresponding plane at 31.7° (211), 46.7° (222), and 25.8° (002) (JCPDS 090432) represents the hexagonal HAp. The peak intensity of the sample decrease as the concentration of chondroitin 4–sulphate increases. The irregular increase in crystallite size is observed because of the swelling behaviour of chitosan and chondroitin 4–sulphate and the formation of apatite layer [43].

FT-IR spectra shown in Fig. 2*b* denote the formation of apatite layer. The peaks observed at 1415 cm^{-1} correspond to Co_3^{2-} indicates the formation of HAp layer [44]. The characteristic such as 1735 and 1255 cm^{-1} reveals $C=O$ stretching and C-N stretching respectively. The peaks observed at in the range of 400–500 cm^{-1} indicates the presence of phosphate groups and hence, these results confirms the CTC nanocomposites possess high bioactivity.

The dry weight of the nanocomposites is measured after 21 days of immersion in 1.5 SBF solution. The weight of the sample is increased due to the swelling behaviour of chitosan and chondroitin 4–sulphate and their ionic interactions [26]. This weight modulation denotes the degrading ability of the

Table 1 As the concentration of chondroitin 4–sulphate increases the particle size decreases are shown in Table 1

Sample name	Concentration of chondroitin 4–sulphate, g/l	Crystallite size, nm	Particle size, nm
CTC 1	0.125	4.18	38.72
CTC 2	0.25	4.08	32.47
CTC 3	0.5	8.05	25.32

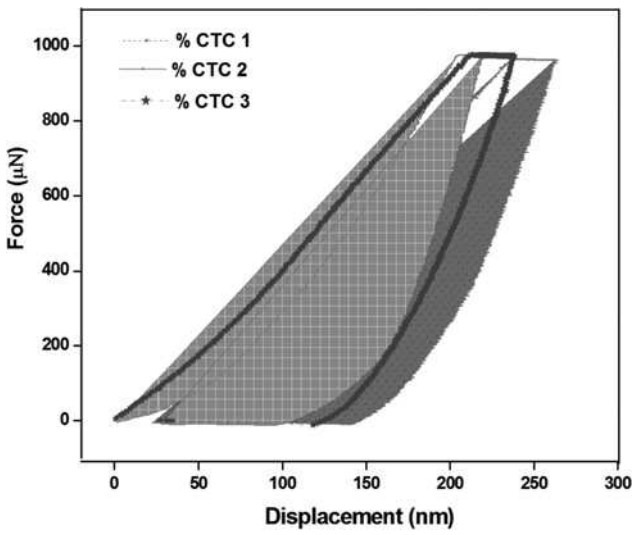

Fig. 5 *Nanoindentation of TiO_2-chitosan- chondroitin 4–sulphate nanocomposite*

Table 2 Percentage of calcium and phosphate in TiO_2-chitosan-chondroitin 4–sulphate nanocomposite

Sample	Ca, %	P, %	Ca/P ratio
CTC 1	2.473	1.465	1.688
CTC 2	2.477	1.674	1.479
CTC 3	5.986	3.455	1.732

nanocomposites. The presence of calcium and phosphate on the surface of the sample is obtained from the XRF results. The Ca/P ratio is calculated and given in Table 2. The Ca/p ratio increases as the concentration of the chondroitin sulphate increases. Thus the CTC nanocomposites possess high bioactivity and suitable for bone implant applications.

3.7 Swelling study

The swelling ability of the CTC nanocomposites after immersing the sample in PBS is shown in the Table 3. The swelling percentage of the nanocomposites at the predetermined days is obtained from their wet weight. As the concentration of the chondroitin 4–sulphate increases, the swelling capacity increases due to the swelling ability of the chondroitin 4–sulphate [45]. The ratio of the sample increases gradually and reaches the maximum on the day 7. The CTC 3 nanocomposites shows maximum swelling ratio of 28.12% and hence, suitable for various biomedical applications.

3.8 Antimicrobial study

The antimicrobial effect of the sample against the *S. aureus* and *E. coli* is evaluated and the zone of inhibition is shown in Table 3. CTC nanocomposites show good antimicrobial effects against gram positive and gram negative bacteria. The clear zone formation around the disc indicates the bacterial inhibition. The diameter of zone of inhibition is different for the different concentration of chondroitin 4–sulphate. The maximum antimicrobial activity is observed in *S. aureus* compared with that of *E. coli*. The CTC 3 nanocomposite shows highly increased antimicrobial activity against *S. aureus* and *E. coli* and is suitable for bone implant applications.

3.9 Biocompatibility study

The biocompatibility and cytotoxic effects of the prepared nanocomposites are evaluated in the human MG 63 cell lines in different concentrations namely 31.25, 65.5, 125, 250 μg ml^{-1} and are shown in Fig. 6. The high concentration (250 μg ml^{-1}) of the nanosample dosages decreases the viability in all CTC nanocomposites due to the overdose effect [40]. The significant increase in cell viability is observed in CTC 1 nanocomposite due to its high surface to volume ratio and its swelling behaviour. Whereas CTC 2 and CTC 3 decrease the cell viability gradually to the higher concentration. However, the toxic effects of the nanocomposites are collectively not significant, which is subsequently proved by the ANOVA statistical analysis. As in the previous studies [41], this study also confirms that the physic-chemical properties play a major role in biological activity. In addition, this study confirms the CTC 1 is the optimal ratio of chitosan, TiO_2 and chondroitin 4–sulphate for the bone implant applications.

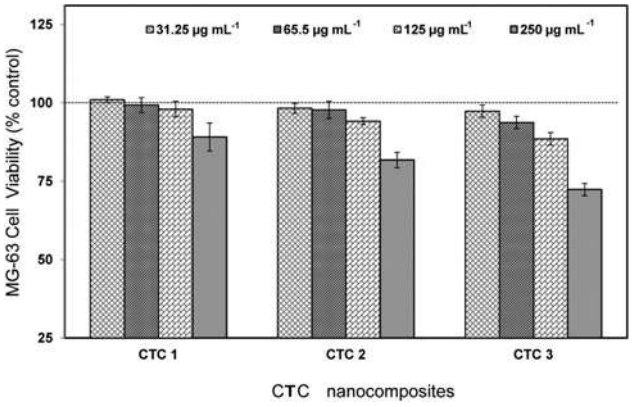

Fig. 6 *Cytotoxicity analysis of TiO_2-chitosan- chondroitin 4–sulphate nanocomposite*

4 Conclusion

The TiO_2-CH-CS nanocomposites were synthesised by *in situ* sol–gel method and characterised by different techniques to explore the particle size, morphology and mechanical stability of the nanocomposites. the antibacterial activity bioactivity swelling nature of the nanocomposite increases as the concentration of the chondroitin 4–sulphate increases whereas the hardness and the biocompatability results reveals that the CTC 1 nanocomposites is the suitable material for the bone implant applications.

5 References

1 Williams, D.: 'Benefits and risk in tissue engineering', *Mater. Today*, 2004, **7**, pp. 9–24
2 Facca, S., Ferrand, A., Palomares, C.M., *et al.*: 'Bone formation induced by growth factors embedded into the nanostructured particles', *J. Biomed. Nanotechnol.*, 2011, **7**, pp. 482–485
3 Jayakumar, R., Roshni, R., Sudheesh Kumar, P.T., *et al.*: 'Fabrication of chitin–chitosan/nano ZrO2 composite scaffolds for tissue engineering applications', *Int. J. Biol. Macromol.*, 2011, **49**, pp. 274–280
4 Yen Lin, C., Hsiao Ping, L., Hing Yuen, C., *et al.*: 'Composite chondroitin-6-sulfate/dermatan sulfate/chitosan scaffolds for cartilage tissue engineering', *Biomaterials*, 2007, **28**, pp. 2294–2305
5 Li, Z., Jiang, C., Wanyin, Z.: 'Preparation and HL-7702 cell functionality of titania/chitosan composite scaffolds', *J. Mater. Sci: Mater. Med.*, 2009, **20**, pp. 949–957
6 Xuanyong, L., Paul Chu, K., *et al.*: 'Surface modification of tanium, titanium alloys, and related materials for biomedical applications', *J. Mater. Sci. Eng., R.*, 2004, **47**, pp. 49–121
7 Venkatesan, J., Se Kwon, K.: 'Chitosan composites for bone tissue engineering', *Marine. Drugs*, 2010, **8**, pp. 2252–2266
8 Ming kung, Y., Kuang ming, C., Chieh shen, H., *et al.*: 'Novel protein-loaded chondroitin sulfate–chitosan nanoparticles: Preparation and characterization', *Acta. Biomater.*, 2011, **7**, pp. 3804–3812
9 Vítor Santo, E., Rita, A., Duarte, C., *et al.*: 'Hybrid 3D structure of poly(d,l-lactic acid) loaded with chitosan/chondroitin sulfate nanoparticles to be used as carriers for biomacromolecules in tissue engineering', *J. Supercritical Fluids*, 2010, **54**, pp. 320–327
10 Maria de la, F., Begon, S., Maria Alonso, J.: 'Novel hyaluronic acid-chitosan nanoparticles for ocular gene therapy', *Invest. Ophthalmol. Vis. Sci.*, 2008, **49**, pp. 2016–2024

Table 3 *In vitro* bioactivity, swelling capacity and antibacterial activity of TiO_2-chitosan-chondroitin 4–sulphate nanocomposites

Sample	After *in vitro* 1.5 SBF study		Swelling weight in PBS			Zone of inhibition, mm	
	Weight modulation, %	Crystalline size, nm	1st day, %	4nd day, %	7th day, %	*S. aureus*	*E. coli*
CTC 1	10.38	85.64	21.42	22.54	26.6	15	8
CTC 2	21.6	81.41	12.51	15.36	17.8	18	12
CTC 3	25	67.26	22.30	24.25	30.12	22	15

11 Fisher, J.P., Reddi, A.H.: 'Functional tissue engineering of bone: signals and scaffolds', in Ashammakhi, N., Ferretti, P. (EDs.): 'Topics in Tissue Engineering' (University of Oulu, 2003), pp. 1–29
12 Hua, D., Cheuk, K., Wei ning, Z., *et al*.: 'Low temperatuire preparation of nano TiO_2 and its applications as antibacterial agents', *Trans. Nonferr. Met. Soc. China*, 2007, **17**, pp. 700–703
13 Manero, J.M., Salsench, J., Noqueras, J., *et al*.: 'Growth of bioactive surface dental implants', *Implant. Dent.*, 2002, **11**, pp. 170–175
14 Ramalingam, S., Muralidharan, V.S., Subramania, A.: 'Electrodeposition and characterization of Cu-TiO_2 nanocomposite coatings', *J. Solid State Electrochem.*, 2009, **13**, pp. 1777–1783
15 Luo, Y.B., Wang, X.L., Xu, D.Y., *et al*.: 'Preparation and characterization of poly (lactic acid)-grafted TiO2 nanoparticles with improved dispersions', *Appl. Surf. Sci.*, 2009, **255**, pp. 6795–6801
16 Suh, J.K., Matthew, H.W.: 'Applications of chitosan based polysaccharides biomaterials in cartilage tissue engineering a review', *Biomaterials*, 2000, **21**, pp. 2589–2598
17 Ho, M.H., Wang, D.M., Hsieh, H.J., *et al*.: 'Preparation and characterization of RGD immbolised chitosan scaffolds', *Biomaterials*, 2005, **26**, pp. 3197–3206
18 Morimoto, M., Saimoto, H., Usui, H., *et al*.: 'Biological activities of carbohydrate branched chitosan derivaties', *Biomacromolecules*, 2001, **2**, pp. 1133–1136
19 Smriti Sharma Vivek, P., Soni Jayesh Bellare, R.: 'Chitosan reinforced apatite–ollastonite coating by electrophoretic deposition on titanium implants', *J. Mater. Sci: Mater. Med.*, 2009, **20**, pp. 1427–1436
20 Singla, A.K., Chawla, M.: 'Chitosan: some pharmaceutical and biological aspects —an update', *J. Pharm. Pharmacol.*, 2001, **53**, pp. 1047–1067
21 Di Martino, A., Sitting, M., Risbud, M.V.: 'Chitosan a versatile bioipolymer for orthopaedic tissue engineering', *Biomaterials*, 2005, **26**, pp. 5983–5990
22 Yang, W., Fu, J., Wang, T., *et al*.: 'Chitosan/sodium tripolyphosphate nanoparticles: Preparation, characterization and application as drug carrier', *J. Biomed. Nanotechnol.*, 2009, **5**, pp. 591–595
23 Peter, M., Nitya, N., Selvamurugan, S.V., *et al*.: 'Preparation and characterization of chitosan-gelatin/nano hydroxyapatite composite scaffolds for tissue engineering applications', *Carbohydr. Polym.*, 2010, **80**, pp. 687–694
24 Ma, L., Gao, C.Y., Mao, Z.W., *et al*.: 'Collagen/chitosan porous scaffolds with improved biostability for skin tissue engineering', *Biomaterials*, 2003, **24**, pp. 4833–4841
25 Lin, Y.S., Okamoto, Y., Minami, S.: 'Effects of chitosan carboxymethyl dextran nanoparticles on cell proliferation and on serum cytokine regulation', *J. Biomed. Nanotechnol.*, 2010, **6**, pp. 247–253
26 Yuan, N.Y., Tsai, R.Y., Ho, M.H., *et al*.: 'Fabrication and characterization of chondroitin sulfate modified chitosan membranes for biomedical applications', *Desalination*, 2008, **234**, pp. 166–174
27 Iouv, M., Dumais, G., Du Souich, P.: 'Anti-inflammatory activity of chondroitin sulfate', *Osteoarthritis Cartilage*, 2008, **16**, pp. 14–18
28 Park, Y.J., Lee, Y.M., Lee, J.Y., *et al*.: 'Controlled release of platelet derived growth factor-BB from chondroitin sulphate–chitosan sponge for guided bone regeneration', *J. Control. Release*, 2000, **67**, pp. 385–394
29 Mi, F.L., Shyu, S.S., Peng, C.K., *et al*.: 'Fabrication of chondroitin sulphate–chitosan composite artificial extracellular matrix for stabilization of fibroblast growth factor', *J. Biomed. Mater. Res.*, 2006, **76**, pp. 1–15
30 Ganza Gonzalez, A., Anguiano Igea, S., Otero Espinar, F.J., *et al*.: 'Chitosan and chondroitin microspheres for oral-administration controlled release of metoclopramide', *Eur. J. Pharm. Biopharm.*, 1999, **48**, pp. 149–155
31 Bjornson, A., Moses, J., Ingemansson, A., *et al*.: 'Primary human glomerular endothelial cells produce proteoglycans, and puromycin affects their posttranslational modification', *Am. J. Physiol. Renal. Physiol.*, 2005, **288**, pp. 748–756
32 Vona, M.L.D., Ahmed, Z., Bellitto, S., *et al*.: 'TiO_2 nanocomposite hybrid proton conductive membranes via *in situ* mixed sol-gel process', *J. Membr. Sci.*, 2007, **296**, pp. 156–161
33 Kavitha, K., Suths, S., Prabhu, M., *et al*.: 'In-situ synthesized novel biocompatible titania-chitosan nanocomposites with high surface area and antibacterial activity', *Carbohydr. Polym.*, 2013, **93**, pp. 731–739
34 Kavitha, K., Prabhu, M., Rajendran, V., *et al*.: 'Optimization of nano-titania and titania-chitosan nanocomposites to enhance the biocompatibility', *Current Nanotechnol.*, 2013, **9**, pp. 308–317
35 Yang, D., Li, J., Jiang, Z., *et al*.: 'Chitosan/TiO_2 nanocomposite pervaporation membranes for ethanol dehydration', *Chem. Eng. Sci.*, 2009, **64**, pp. 3130–3137
36 Amin, K.A.M., Panhuis, M.I.H.: 'Reinforced materials based on chitosan TiO_2 and Ag composites', *Polymers*, 2012, **4**, pp. 590–599
37 KoKubo, T., Takadama, H.: 'How useful is SBF in predicting in vivo bone bioactivity?', *Biomaterials*, 2006, **27**, pp. 2907–2915
38 Jian kang, H., Dichen, L., Yaxiong, L., *et al*.: 'Preparation of chitosan-gelatin hybrid scaffolds with well-organized microstructures for hepatic tissue engineering', *Acta. Biomater.*, 2009, **5**, pp. 453–461
39 Joana, M., Na, Y., Sofia Caridade, G., *et al*.: 'Chitosan/bioactive glass nanoparticle composite membranes for periodontal regeneration', *Acta. Biomater.*, 2012, **8**, pp. 4173–4180
40 Jing, H., Xiong, G., Yanxia, L., *et al*.: 'Synthesis and characterization of selenium–chondroitin sulfate nanoparticles', *Carbohydr. Polym.*, 2012, **90**, pp. 122–126
41 Jayachandran, V., Ramjee, P., Ira, B., *et al*.: 'Chitosan–amylopectin/hydroxyapatite and chitosan–chondroitin sulphate/hydroxyapatite composite scaffolds for bone tissue engineering', *Int. J. Biol. Macromol.*, 2012, **51**, pp. 1033–1042
42 Kavya, K.C., Rachna, D., Jayakumar, R., *et al*.: 'Synthesis and characterization of chitosan/chondroitin sulfate/nano-SiO2 composite scaffold for bone tissue engineering', *J. Biomed. Nanotechnol.*, 2012, **8**, pp. 149–160
43 Jiang, L., Li, Y., Wang, X., *et al*.: 'Preparation and properties of nano-hydroxiapatite/chitosan/carboxymethyl cellulose composite scaffold', *Carbohydr. Polym.*, 2008, **74**, pp. 680–684
44 Markovic, M., Fowler, B.O., Tung, M.S.: 'Preparation and comprehensive characterization of a calcium hyroxy apatite', *J. Res. Natl. Inst. Stand. Technol.*, 2004, **109**, pp. 553–568
45 Jing, H., Xiong, G., Yanxia, L., *et al*.: 'Synthesis and characterization of selenium–chondroitin sulfate nanoparticles', *Carbohydr. Polym.*, 2012, **90**, pp. 122–126